2010 IEEE International Conference on Robotics and Automation
Anchorage Convention District
May 3-8, 2010, Anchorage, Alaska, USA

Adaptive Exploitation of Multipath Fading for Mobile Sensors

Magnus Lindhé and Karl Henrik Johansson

Abstract— **Mobile wireless sensors in indoor environments will experience multipath fading, causing rapid variations in the capacity of the radio link. We present a strategy that increases the throughput by modifying the trajectory of the sensor so it spends more time at positions where the capacity is high. While doing so, it still maintains some desired average velocity. Our approach includes closed-loop estimation of the parameters of the fading, which may change when moving between rooms. We prove stability of the feedback system and illustrate its behavior through simulations. Finally, we demonstrate robustness to errors in the channel model.**

I. Introduction

There is growing awareness that the communication channel must be taken into account when coordinating mobile sensor networks. Avoiding physical obstacles has a long tradition in robotics, but there is an equally real but invisible radio propagation environment that needs to be taken into consideration. Successful sensing requires both reaching the desired location *and* transferring sensor information to the recipient.

The interaction of motion and communication can be modeled in different ways, depending on what radio propagation phenomena dominate in a particular environment and what kinds of analysis the model must allow. Path loss, shadowing and multipath fading are three important such phenomena, briefly described below.

In open fields or in long distance deployments, the *distance-dependent path loss* dominates. Some model this as circular regions of perfect coverage and others as the signal gradually decreasing with distance. This allows joint optimization of sensing and communication objectives [1], [2]. Such models can also be used to develop algorithms with guaranteed connectivity within the group [3].

When obstacles are present, *shadowing* will occur, *i.e.*, attenuation of the signal as it passes through an obstacle. Shadowing can be avoided by requiring a direct line of sight, which gives the motion planning problem a more geometric nature [4], [5].

In indoor or urban settings, *multipath fading* becomes significant. It is caused by negative or positive interference from multiple reflections of the same signal, and results in signal strength variations over distances that are just a fraction of a wavelength. Since the fading has a complex dependence on the layout of the environment, it is usually treated as a stochastic effect. Even small movements of a sensor node will change the fading, which can be exploited to improve the signal strength for a stationary sensor node [6]. If the node is connected in a network, such small movements will change the capacities of the different links, which may be used for load balancing [7]. Estimating the spatial correlation of the fading can also give important information. Mobile sensors can adapt the step size of their movement so as to faster escape from deep fades [8].

The main contribution of this paper is a novel adaptive architecture that closes the loop between motion and communication in environments with multipath fading. We study a robot moving along a reference trajectory, adapting its motion so as to spend more time at positions where the signal strength is high. We have previously shown that such stop-and-go motion improves the average radio throughput [9]. By applying feedback from the robot position, we can improve those results, maintaining tracking of the reference position and making the system adapt to varying channel parameters.

The analysis includes proofs of input-output stability of the closed-loop system, as well as convergence in the absence of noise. Moreover, we illustrate how the feedback architecture gives robustness to errors in the channel model, which are likely to occur in practical usage. Finally, we discuss how to tune the time constant of the channel estimator, which is a matter of separation of time scales between the stop-and-go motion and the estimator dynamics.

In the following section, we introduce models for the motion and communication and formulate the problem. In Section III, we briefly recapitulate the stop-and-go motion for completeness. Section IV presents the proposed architecture and an analysis of its stability and time constant. Simulations in Section V illustrate how the feedback improves the performance of the system and its robustness. Finally there is a short conclusion.

II. Problem Formulation

Fig. 1 shows the problem scenario. We consider a robot following a reference trajectory in an environment with multipath fading. It makes regular stops and measures the signal strength to determine how long each stop should last. By stopping longer at points with high signal strength, we can improve the total throughput while still making sure that the robot tracks the reference within some margin. We give a model for the fading channel as well as the motion of the robot and end by formally stating the problem of finding a *stop-time policy*.

This work was partially supported by the Swedish Defence Materiel Administration (FMV) through the TAIS programme 297316-LB704859, the Swedish Research Council and the Swedish Foundation for Strategic Research.

The authors are with the ACCESS Linnaeus Centre, School of Electrical Engineering, Royal Institute of Technology, SE-100 44 Stockholm, Sweden {lindhe|kallej}@ee.kth.se

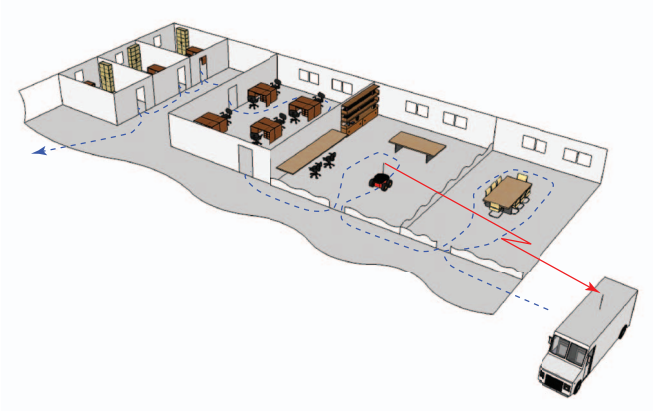

Fig. 1. A robot is following a reference trajectory while sending sensor information to a base station. Reflections off walls and furniture cause multipath fading, which makes the radio signal strength fluctuate. By stopping periodically and making longer stops at positions with high signal strength, the robot can increase the link throughput. On average, the robot still tracks the reference position.

A. Communication Model

This section presents some communication preliminaries that will be needed for understanding the analysis of the proposed strategy. Our communication model is based on the popular Tmote Sky sensor board, which implements IEEE 802.15.4, communicates at 2.4 GHz and uses quadrature phase shift keying (QPSK) modulation [10]. The bit error rate (BER) for QPSK for a signal with signal-to-noise ratio (SNR) γ is [11, p. 223]

$$P_b(\gamma) = Q(\sqrt{\gamma}),$$

where $Q(x)$ is the cumulative distribution function of the standard normal distribution.

We define the link capacity as the packet reception rate. Under the assumption of bit-to-bit error independence, the capacity is

$$c(\gamma) = c_0[1 - Q(\sqrt{\gamma})]^{8N},$$

where N is the number of bytes in a package and c_0 is the nominal capacity. IEEE 802.15.4 defines a packet length of 11 bytes, plus address and payload. With an address and payload of 4+8 bytes, the Tmote has a nominal capacity of 1360 packets/s.

We further assume static Rayleigh fading. By this we mean that the channel is Rayleigh fading, but the environment is static so the fading does not change over time if the robot stands still. It is exponentially distributed:

$$f_\gamma(\gamma) = \frac{1}{\Gamma} e^{-\gamma/\Gamma}, \tag{1}$$

where Γ is the average SNR. The spatial autocorrelation of γ has a zero at the inter-sample distance of 0.38 wavelengths of the carrier signal, which is 4.75 cm at 2.4 GHz. In practice, two samples are often considered independent if the inter-sample distance is greater than half a wavelength [12].

Since the Tmote has a 1 MHz bandwidth, we consider the fading to be flat. Further, the robot is assumed to only move at walking speeds, so even when it is moving, the fading is slow [11]. (Meaning that the channel is considered constant over the duration of one bit.)

B. Robot Model

We study one-dimensional movement along a pre-defined reference trajectory, where the reference position moves with velocity v_{ref}. The relative position of the robot is $\Delta(t)$, where $\Delta > 0$ means that the robot is ahead of the reference, and we assume $\Delta(0) = 0$. The robot first drives at velocity v_d for a constant time τ_d, then stops, samples γ and stands still for a time $\tau_s(\gamma)$ before starting over again. Formally, we define the system dynamics as

$$\dot{\Delta}(t) = \begin{cases} -v_{\text{ref}} \text{ when } t_k \le t < t_k + \tau_s(\gamma[k]) \\ v_d - v_{\text{ref}} \text{ else,} \end{cases} \tag{2}$$

for all $k \ge 0$, where

$$t_k = k\tau_d + \sum_{m=1}^{k} \tau_s(\gamma[m-1]) \tag{3}$$

and $\gamma[k]$ denotes the SNR, sampled at time t_k.

Note that if $v_d\tau_d$ is greater than half a wavelength, which is 6.3 cm for a 2.4 GHz signal, we can consider all $\gamma[k]$ as if they are independent. Also note that we only sample the SNR when standing still. This allows us to estimate the signal strength over several received packets, which is often necessary for low-cost transceivers because the signal strength sensor is inaccurate.

C. Problem Formulation

For the stochastic hybrid system (2), where independent samples $\gamma[k]$ are drawn from the distribution (1), find a stop-time policy $\tau_s(\gamma)$ that yields the average velocity v_{ref} and compute the resulting average link capacity.

We will first restate our solution from [9] for the case when the average SNR Γ is known, and then study the case when it has to be estimated on-line.

III. Solution for Known Average SNR

Assuming that the average SNR Γ is known, we propose a stop-time policy and analyze the resulting link capacity it yields.

A. Stop-Time Policy

We propose a simple threshold policy: After sampling the SNR, the robot stands still for a fixed time $\alpha\tau_d$ if the SNR is above some threshold γ_{th}, otherwise it immediately resumes driving. The choice of $\alpha > 0$ will be discussed later in this section. The policy can formally be stated as

$$\tau_s(\gamma) = \begin{cases} \alpha\tau_d \text{ if } \gamma > \gamma_{th} \\ 0 \text{ else.} \end{cases} \tag{4}$$

The average velocity after $M+1$ stop-and-go cycles is

$$\frac{\sum_{k=0}^{M} v_d\tau_d}{\sum_{k=0}^{M}(\tau_d + \tau_s(\gamma[k]))}.$$

As $M \to \infty$, we get the expected velocity as

$$E\{v\} = \frac{v_d \tau_d}{\tau_d + E\{\tau_s\}}.$$

The expected stop-time can be computed as

$$E\{\tau_s\} = \int_{\gamma_{th}}^{\infty} \alpha\tau_d \frac{1}{\Gamma} e^{-\gamma/\Gamma} \mathrm{d}\gamma = \alpha\tau_d e^{-\gamma_{th}/\Gamma}. \quad (5)$$

Since $\gamma_{th} < 0$ has the same effect as $\gamma_{th} = 0$, this shows that $\alpha\tau_d$ is a lower bound for the average stop time. In the following, we will assume $\alpha > 1$ and use $\gamma_{th} = \Gamma \ln \alpha$, which yields $E\{\tau_s\} = \tau_d$ and $E\{v\} = \frac{1}{2} v_d$.

High values of α correspond to making very few stops at positions with high SNR. But such a policy causes very large deviations from the reference position. It also depends on the Rayleigh distribution being an accurate channel model also at very high SNR, which is not the case. The extreme case $\alpha \to \infty$ represents making a single stop at a position with infinite SNR, which is physically impossible since for a given noise level, the SNR is limited by the transmitted signal power. It is, however, easy to see that this pathological case corresponds to the maximum expected link capacity. On the other hand, small values of α limit the time the robot can spend at really good positions and thus reduces the achievable link capacity. In experiments, we have found $\alpha = 4$ to be a reasonable compromise.

B. Expected Link Capacity

With the choice of parameter shown above and by letting $v_d = 2v_{\text{ref}}$, the expected velocity of the robot will equal the reference velocity. We will now analyze the expected average link capacity.

While driving, the robot experiences slow fading and the average driving capacity c_d is

$$c_d \triangleq c_0 \int_0^{\infty} [1 - Q(\sqrt{\gamma})]^{8N} \frac{1}{\Gamma} e^{-\gamma/\Gamma} \mathrm{d}\gamma.$$

We then compute the expected amount of data transmitted per stop:

$$E\{c\tau_s\} = \int_0^{\infty} c(\gamma)\tau_s(\gamma) f_\gamma(\gamma) \mathrm{d}\gamma$$

The average link capacity for $M+1$ stop-and-go cycles can be computed as

$$\frac{\sum_{k=0}^{M} \left(c(\gamma[k])\tau_s(\gamma[k]) + c_d\tau_d\right)}{\sum_{k=0}^{M} \left(\tau_s(\gamma[k]) + \tau_d\right)}.$$

In the limit as $M \to \infty$, we get the expected average link capacity as

$$E\{c\} = \frac{E\{c\tau_s\} + c_d\tau_d}{2\tau_d}.$$

The resulting link capacity is depicted in Fig. 2. For comparison, we have also included the capacity c_d when driving at constant velocity. This is the same capacity as would be obtained by the constant policy $\tau_s(\gamma) \equiv \tau_d$. Using the proposed stop-and-go motion yields over 50% more capacity than constant velocity when $\Gamma < 7$ dB. The prize we pay for this capacity improvement is some deviation from the reference position.

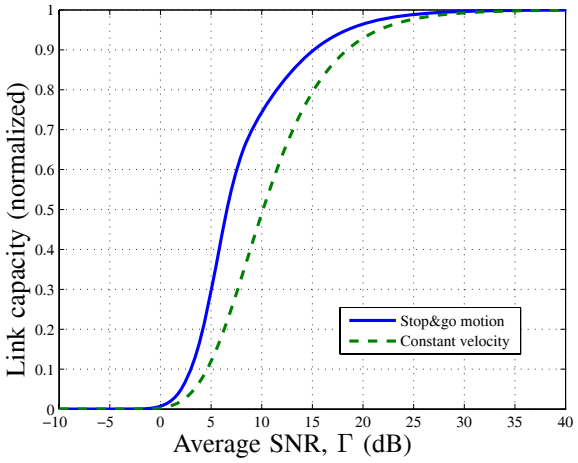

Fig. 2. Expected link capacity (*i.e.*, packet reception ratio) as a function of the average SNR Γ. Using the stop-and-go motion is particularly beneficial in the transition region, where the signal is weak but still detectable.

IV. Estimating Channel Parameters

So far we have assumed that the average SNR Γ is constant and known. In practice, Γ depends on the output power of the transmitter, the path loss and the noise level. When the robot is moving over larger distances, the shadowing due to obstacles between transmitter and receiver can be expected to vary, which changes the path loss. Therefore, we propose a feedback scheme to compute an estimate $\hat{\Gamma}$ of Γ.

If $\hat{\Gamma}$ underestimates Γ, the robot will stop too often and thus fall behind the reference. The opposite happens if $\hat{\Gamma}$ overestimates Γ. By monitoring the relative position $\Delta(t)$, a controller can adjust $\hat{\Gamma}$ to match the current channel properties. The controller is formulated in discrete time, sampling $\Delta(t)$ irregularly at each instant t_k. We first define the closed-loop system and then show that the SNR estimate will converge to Γ and the relative position to zero.

A. Closed-Loop Estimation

Our model of the system with an estimator is illustrated in Fig. 3. The SNR estimate in dB, $u[k] \triangleq 10 \log \hat{\Gamma}(t_k)$ is the input to the robot, which has dynamics (2) and follows the policy $\tau_s(\gamma)$. We also define $d[k]$ as the change in relative position during the interval $t_k \le t < t_{k+1}$, thus the relative position at time t_k is

$$\Delta[k] = \Delta[k-1] + d[k-1].$$

Due to our probabilistic model of the fading, the position change is considered stochastic. As we will show later, the expected value of $d[k]$ is a function of the SNR estimate. We define it as

$$f(u[k]) \triangleq E\{d[k]\}.$$

The deviation from the expectation will be white noise since we consider all samples $\gamma[k]$ as independent. We denote it $w[k]$:

$$w[k] = d[k] - E\{d[k]\}$$

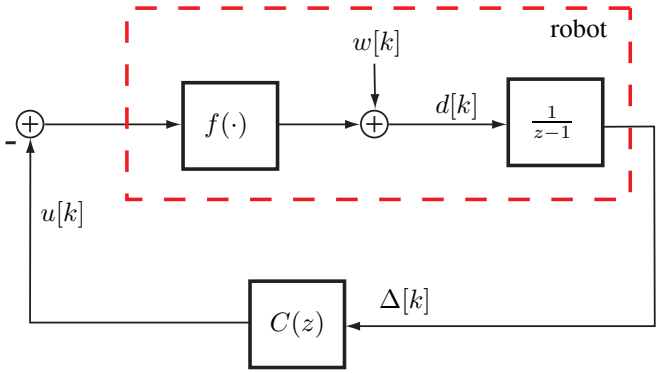

Fig. 3. The controller $C(z)$ uses u, the SNR estimate in dB, to control the average motion of the robot. It uses the relative position Δ, as input.

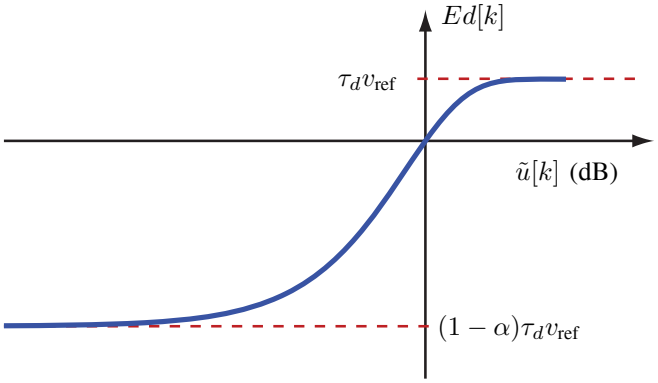

Fig. 4. The static nonlinearity $\tilde{g}$, giving the expected change of relative position per sampling period, as a function of the SNR estimation error.

Note that since the stop times have an upper bound, $d[k]$ and hence the noise $w[k]$ are also bounded.

This architecture allows us to introduce a controller $C(z)$, which uses $u[k]$ to control the relative position $\Delta[k]$.

B. Static Nonlinearity

Here we give expressions for the static nonlinearity f. The change in relative position at each stop-and-go cycle is

$$d[k] = \tau_d v_d - (\tau_d + \tau_s(\gamma[k]))\, v_{\text{ref}},$$

so

$$E\{d[k]\} = \tau_d(v_d - v_{\text{ref}}) - v_{\text{ref}} \int_0^\infty \tau_s(\gamma) f_\gamma(\gamma) \mathrm{d}\gamma.$$

For the policy (4), the nonlinearity becomes

$$f(u[k]) = E\{d[k]\} = \tau_d \left(v_d - v_{\text{ref}} - v_{\text{ref}} \alpha^{(1-\hat{\Gamma}/\Gamma)} \right).$$

Note that this does not depend on the actual values of Γ and $\hat{\Gamma}$, only the ratio. This motivates a change of control variable to $\tilde{u}[k]$, which we define as the relative SNR estimation error in dB:

$$\tilde{u}[k] \triangleq 10 \log \frac{\hat{\Gamma}}{\Gamma} = u[k] - 10 \log \Gamma \tag{6}$$

We also define the static nonlinearity

$$g(\tilde{u}[k]) = f(\tilde{u}[k] + 10 \log \Gamma) + k_{\min} \tilde{u}[k].$$

The last term is included for technical reasons, to ensure a minimum slope of $k_{\min}$. This term can be introduced by letting the (previously constant) driving velocity v_d vary slightly with the SNR:

$$v(\gamma) = v_d - \frac{10 k_{\min}}{\tau_d} \kappa \log e - \frac{k_{\min}}{\tau_d} 10 \log \frac{\gamma}{\Gamma},$$

where $\kappa \approx 0.577$ is Euler's constant. This is not used in the simulations, but is required for the stability proof below, to ensure global convergence of the estimator even for very large initial estimation errors.

The maximum slope of g is

$$k_{\max} \triangleq \max_{\tilde{u}} \frac{\mathrm{d}g}{\mathrm{d}\tilde{u}} = \tau_d v_{\text{ref}} \frac{\ln 10}{10} \alpha^{(1-1/\ln \alpha)} + k_{\min}.$$

C. State Space Description

We propose a PI-controller with proportional gain k_P and integral gain k_I. The closed-loop system can then be described on state space form as

$$\begin{aligned} x[k+1] &= \underbrace{\begin{bmatrix} 1 & 1 \\ 0 & 1 \end{bmatrix}}_{A} x[k] + \underbrace{\begin{bmatrix} 0 \\ 1 \end{bmatrix}}_{B} d[k] \\ \tilde{u}[k] &= \underbrace{\begin{bmatrix} k_I & k_P \end{bmatrix}}_{C} x[k] \\ d[k] &= g(-\tilde{u}[k]) + w[k]. \end{aligned} \tag{7}$$

D. Closed-Loop Stability

We start by showing that the system with input $w[k]$ is l_2 stable. This means that for a bounded noise input $w[k] \in l_2$, we will have a bounded SNR estimation error $\tilde{u}[k] \in l_2$.

Proposition 1 (l_2 stability): Using $k_{\min} = 0.01$, the system (7) with the controller parameters

$$k_P = \frac{2(1-a)}{k_{\min}}, \quad k_I = \frac{(a-1)^2}{k_{\min}},$$

is l_2 stable if

$$\frac{2}{\sqrt{k_{\min}/k_{\max} + 1}} - 1 < a < 1. \tag{8}$$

Proof: We will use the circle criterion [13, Theorem 6.7.37], but first we need to make a loop transformation. Using $k_{\min}$ as a constant gain element, we can define a modified nonlinearity $\tilde{g}$ as

$$\tilde{g}(\tilde{u}[k]) \triangleq g(\tilde{u}[k]) - k_{\min} \tilde{u}[k].$$

This is illustrated in Fig. 4.

The system (7) can then be redrawn as in Fig. 5, where the dashed subsystem $\tilde{G}(z)$ has transfer function

$$\tilde{G}(z) = \frac{2(1-a)z + a^2 - 1}{k_{\min}(a-z)^2}.$$

The system $\tilde{G}(z)$ is stable since it has a double pole in $z = a$ and the nonlinearity $\tilde{g}$ belongs to the sector $[0, k_{\max}]$.

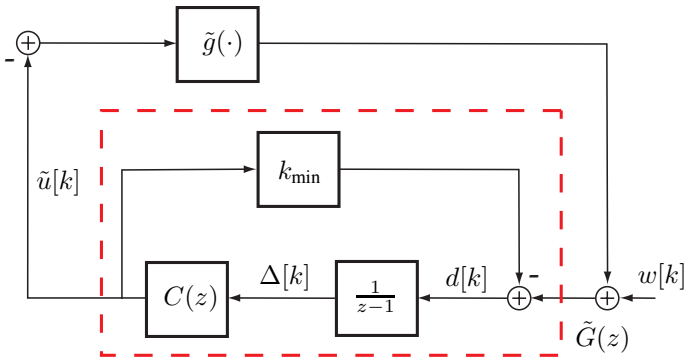

Fig. 5. The closed-loop system after a loop transformation. The dashed subsystem is linear and asymptotically stable and we can apply the circle criterion.

Then, according to the circle criterion, the feedback system is l_2 stable if

$$\mathrm{Re}\{\tilde{G}(z)\} > -1/k_{\max} \ \forall \ |z| = 1. \tag{9}$$

As shown in [14], this is fulfilled if

$$\frac{2}{\sqrt{k_{\min}/k_{\max}+1}} - 1 < a < 1.$$

■

We now consider the case with no noise, $w[k] = 0$. Since $g(0) = 0$, the system (7) has an equilibrium at $x = 0, \tilde{u} = 0$. This corresponds to when there is no deviation from the reference trajectory ($\Delta = 0$) and the SNR estimate is correct.

Corollary 1 (Asymptotic stability): With the choice of controller parameters as in Proposition 1 and if $w[k] = 0 \ \forall \ k$, the system (7) has a globally asymptotically stable equilibrium at $x = 0$.

Proof: The pair (A, B) is controllable and the pair (C, A) is observable since $k_I \neq 0$. Further, the nonlinearity g is Lipschitz continuous. Then the l_2 stability of the forced system (7) implies that $x = 0$ is a globally attractive equilibrium of the system with no input [13, Theorem 6.3.46]. ■

E. Tuning the Time Constant

Proposition 1 allows for a range of pole placements a, which leaves some design freedom to set the time constant of the estimator. A long time constant (a close to 1) makes $\hat{\Gamma}$ less sensitive to noise, but adapting to changes in Γ takes very long. A short time constant (a closer to 0) causes $\hat{\Gamma}$ to vary on the same time scale as the stop-and-go motion, which gives a lower improvement of the link capacity than predicted. The choice must depend on how fast the SNR is expected to vary in the specific application, but when using the parameters described below, we recommend selecting a in the interval $[0.980, 0.997]$, which limits the reduction of the link capacity to a few percent.

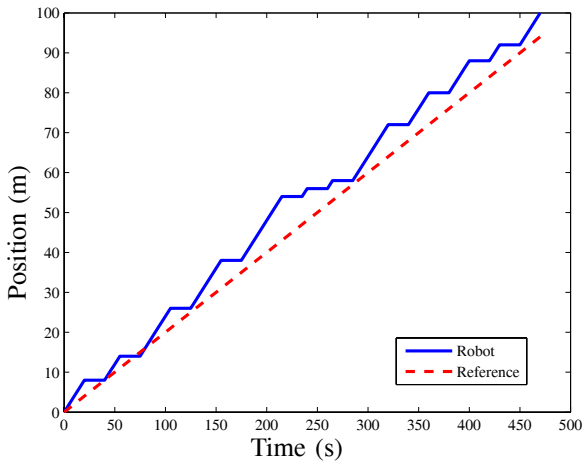

Fig. 6. Stop-and-go trajectory when the average SNR Γ is constant and known.

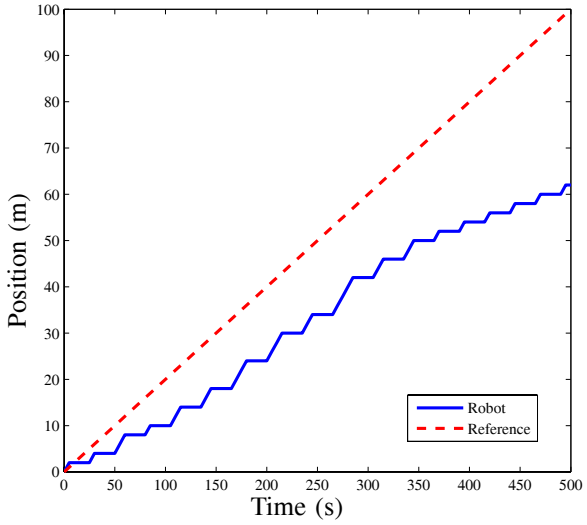

Fig. 7. If the SNR estimate is constantly 3 dB too low, the robot falls behind the reference.

V. Simulations

Here we illustrate the performance of the stop-and-go strategy, both for known channel parameters and when estimating the channel in closed loop. We end by showing that the system is robust to errors in the channel model. All simulations use the following parameters: v_{ref}=0.2 m/s, v_d=0.4 m/s, τ_d=5 s, α=4 and $a = 0.9957$.

A. Running in Open Loop

Fig. 6 illustrates the stop-and-go motion of the system when running in open loop. If the average SNR Γ is known, the robot tracks the reference trajectory. However, if Γ is underestimated by 3 dB, as in Fig. 7, the robot makes too long stops and falls behind the reference. This motivates using the closed-loop estimation.

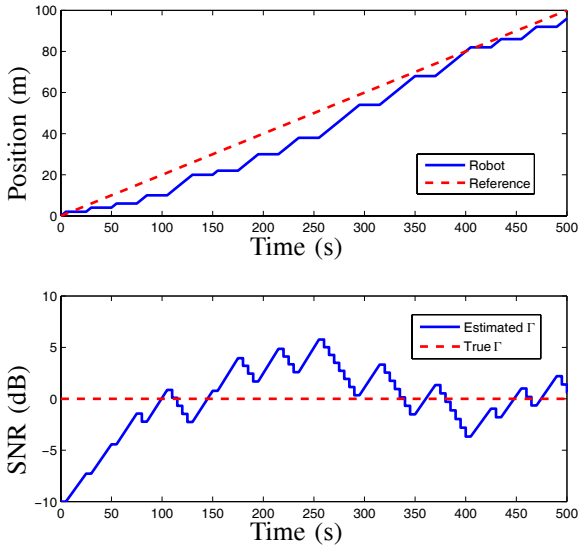

Fig. 8. A simulation of using closed-loop estimation of the average SNR Γ. The initial estimate is too low, so the robot falls behind but then converges to the correct estimate and manages to track the reference position.

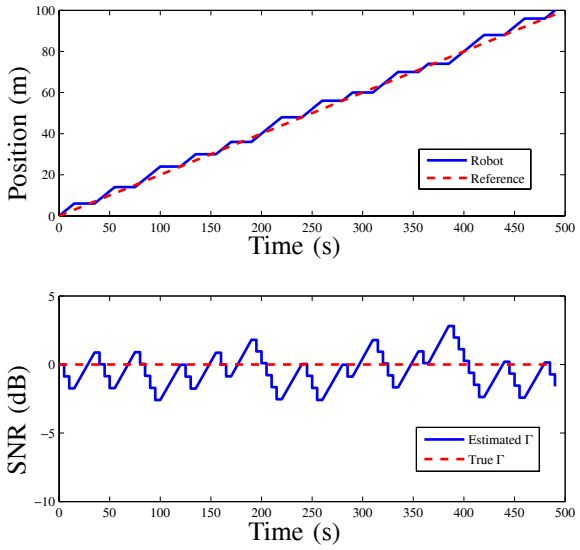

Fig. 9. An illustration of the robustness of the closed-loop system: The fading is now Rice distributed, which causes a slight bias in the SNR estimate $\hat{\Gamma}$, but the robot still tracks the reference trajectory.

B. Closed-Loop Estimation

Here we demonstrate convergence of the closed-loop estimator. The correct average SNR is $\Gamma = 0$ dB, but the initial estimate is $\hat{\Gamma} = -10$ dB. Fig. 8 shows the robot trajectory and the evolution of $\hat{\Gamma}(t)$.

C. Robustness

The derivation above assumes Rayleigh fading, where there is no line of sight between the robot and its base station. If a line of sight component does exist, this may change the distribution of the fading. This is often modeled as a Rice distribution [11]. To illustrate the robustness of the closed-loop system, Fig. 9 shows a simulation where the SNR samples are drawn from the Rice distribution, with a Rice factor of $K = 17$ dB. The error in the channel model causes a slight bias in the SNR estimate, but it does not affect the tracking of the reference trajectory.

VI. Conclusions

We have presented a feedback system that allows a robot to do stop-and-go motion along a reference trajectory to improve its wireless throughput. While doing so, it maintains tracking of the reference position, even if the channel properties vary along the way.

Although the PI-controller is formulated as an estimator, in practice it controls the relative position, so it sacrifices estimation accuracy if needed to correct for faulty initial positions or errors in the SNR distribution. In the case of Rayleigh fading, the control output eventually converges to a correct estimate of the average SNR.

References

[1] T. H. Chung, J. W. Burdick, and R. M. Murray, "A decentralized motion coordination strategy for dynamic target tracking," in *Proceedings of the 2006 IEEE International Conference on Robotics and Automation*, Orlando, USA, 2006.

[2] N. Michael, M. M. Zavlanos, V. Kumar, and G. J. Pappas, "Maintaining connectivity in mobile robot networks," in *Proceedings of the International Symposium on Experimental Robotics*, Athens, Greece, 2008.

[3] D. Dimarogonas and K. J. Kyriakopoulos, "Connectedness preserving distributed swarm aggregation for multiple kinematic robots," *IEEE Transation on Robotics*, vol. 24, no. 5, 2008.

[4] A. Ganguli, J. Cortés, and F. Bullo, "Distributed deployment of asynchronous guards in art galleries," in *American Control Conference*, Minneapolis, USA, 2006.

[5] J. Sweeney, R. Grupen, and P. Shenoy, "Active QoS flow maintenance in controlled mobile networks," in *Proceedings of the Fourth International Symposium on Robotics and Automation*, 2004.

[6] M. Lindhé, K. H. Johansson, and A. Bicchi, "An experimental study of exploiting multipath fading for robot communications," in *Proceedings of Robotics: Science and Systems*, 2007.

[7] D. Puccinelli, M. Brennan, and M. Haenggi, "Reactive sink mobility in wireless sensor networks," in *First ACM Workshop on Mobile Opportunistic Networking*, Puerto Rico, 2007.

[8] Y. Mostofi, "Communication-aware motion planning in fading environments," in *Proceedings of the 2008 IEEE International Conference on Robotics and Automation*, Pasadena, USA, 2008.

[9] M. Lindhé and K. H. Johansson, "Using robot mobility to exploit multipath fading," *IEEE Wireless Communications*, February 2009.

[10] Moteiv Corporation, "Tmote Sky datasheet 1.02," 2006, last visited 2007-05-19. [Online]. Available: http://www.moteiv.com

[11] G. L. Stüber, *Principles of mobile communication*. Kluwer academic publishers, 1996.

[12] W. C. Jakes, Ed., *Microwave Mobile Communications*. IEEE Press, 1974.

[13] M. Vidyasagar, *Nonlinear Systems Analysis*. Prentice-Hall, 1993.

[14] M. Lindhé, "Computing the Nyquist curve for a class of second-order systems," Royal Institute of Technology, Tech. Rep., 2009. [Online]. Available: http://www.ee.kth.se/php/modules/publications/reports/2009/TRITA-EE_2009_055.pdf